Neuronal discrimination capacity

2003 J. Phys. A: Math. Gen. 36 12379

(http://iopscience.iop.org/0305-4470/36/50/003)

INSTITUTE OF PHYSICS PUBLISHING JOURNAL OF PHYSICS A: MATHEMATICAL AND GENERAL

J. Phys. A: Math. Gen. **36** (2003) 12379–12398 PII: S0305-4470(03)61448-4

Neuronal discrimination capacity

Yingchun Deng[1,2], Peter Williams[2], Feng Liu[2,3] and Jianfeng Feng[2]

[1] Department of Mathematics, Hunan Normal University 410081, Changsha, People's Repubic of China
[2] COGS, University of Sussex at Brighton, BN1 9QH, UK
[3] Physics Department, Nanjing University, People's Repubic of China

E-mail: jianfeng@cogs.susx.ac.uk

Received 27 March 2003, in final form 1 September 2003
Published 2 December 2003
Online at stacks.iop.org/JPhysA/36/12379

Abstract

We explore neuronal mechanisms of discriminating between masked signals. It is found that when the correlation between input signals is zero, the output signals are separable if and only if input signals are separable. With positively (negatively) correlated signals, the output signals are separable (mixed) even when input signals are mixed (separable). Exact values of discrimination capacity are obtained for two most interesting cases: the exactly balanced inhibitory and excitatory input case and the uncorrelated input case. Interestingly, the discrimination capacity obtained in these cases is independent of model parameters, input distribution and is universal. Our results also suggest a functional role of inhibitory inputs and correlated inputs or, more generally, the large variability of efferent spike trains observed in *in vivo* experiments: the larger the variability of efferent spike trains, the easier it is to discriminate between masked input signals.

PACS number: 87.19.La

1. Introduction

We present a study on the discrimination capacity of the simplest neuron model: the integrate-and-fire (IF) model. Suppose that a neuron receives two sets of signals. Both of them are contaminated by noise, as shown in figure 1. After neuronal transformations, we want to know whether the signals become more mixed or more separated. This is a typical scenario in decision theory.

We conclude that without correlation between signals, the output histograms are separable if and only if the input histograms are separable. With positively correlated input signals, the output histograms become more separable than input histograms. With negatively correlated input signals, the output histograms are more mixed than input histograms. This is a clear-cut and interesting result. In fact, in recent years, there have been many publications devoted to

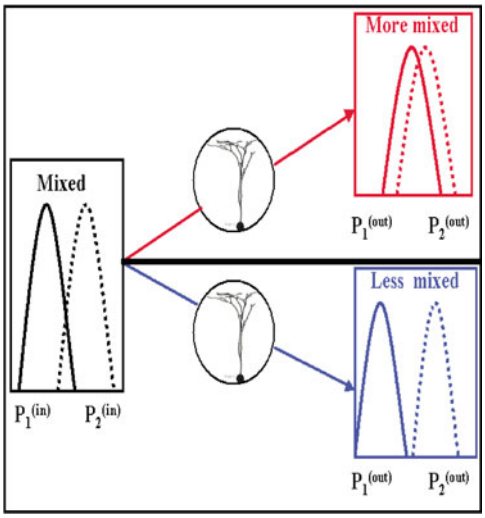

Figure 1. Two possibly mixed input signals, after neuronal transformation. Will they become more separated or more mixed?

exploring the functional role of correlated neuronal activity. For example, synchronization is a special case of correlated neuronal activity [17, 19, 37]. People have extensively investigated the functional roles of correlations in neurons from information theoretic approaches [24, 25, 36], experimental approaches [32, 41] and modelling approaches [1, 6, 33, 34].

In the classical theory of neural networks, we only take into account the excitatory inputs. However, in recent years, we have found many intriguing functional roles of inhibitory inputs, ranging from linearizing the input–output relationship of a neuron [14], to synchronizing a group of neurons [38] and to actually increasing neuron firing rates [9]. In particular, neuronal and neuronal network models with an exactly balanced inhibitory and excitatory input are intensively studied in the literature [30, 39]. For these two most interesting cases, independent input case and exactly balanced input case, we are able to find the exact value of neuronal discrimination capacity. Roughly speaking, here discrimination capacity is the minimal number of synapses carrying signals so that the output histograms of the neuron are separable, provided that input signals are different (see section 3 for the definition). Interestingly, the obtained analytical discrimination capacity is *universal* for the model. It is independent of the decay rate, threshold, magnitude of excitatory postsynaptic potential (EPSP) and inhibitory postsynaptic potential (IPSP), and the input signal distributions.

The paper is organized as follows. In section 2, the model is exactly defined. In section 3, we consider the worst case and the exact value of discrimination capacity is obtained. In section 4, we generalize the results from section 3. In section 5, some numerical results are included. We have presented numerical results for the integrate-and-fire model and the IF–FHN model [9] in a meeting report [10]. In section 6, we briefly discuss related issues. And finally, in the appendix, theoretical proofs of theorems in section 4 and section 5 are presented.

2. The models

The neuron model we use here is the classical integrate-and-fire model [5, 8, 13, 35]. When the membrane potential $V_t^{(k)}$ is below the threshold V_{thre}, it is given by

$$\mathrm{d}V_t^{(k)} = -L\big(V_t^{(k)} - V_{\mathrm{rest}}\big)\,\mathrm{d}t + \mathrm{d}I_{\mathrm{syn}}^{(k)}(t) \tag{1}$$

where L is the decay coefficient and the synaptic input is

$$I_{\mathrm{syn}}^{(k)}(t) = a\sum_{i=1}^{p} E_i^{(k)}(t) - b\sum_{j=1}^{q} I_j^{(k)}(t)$$

with $E_i^{(k)}(t)$, $I_i^{(k)}(t)$ as Poisson processes with rates $\lambda_{i,E}^{(k)}$ and $\lambda_{i,I}^{(k)}$, respectively, $a > 0, b > 0$ are the magnitudes of each EPSP and IPSP, p and q are the total number of active excitatory and inhibitory synapses, $k = 1, 2$ represent different input signals and we aim at discriminating between them in terms of an observation of efferent firing rates. Once $V_t^{(k)}$ crosses V_{thre} from below a spike is generated and $V_t^{(k)}$ is reset to V_{rest}, the resting potential. This model is termed the IF model. The interspike interval of efferent spikes is

$$T^{(k)} = \inf\big\{t : V_t^{(k)} \geqslant V_{\mathrm{thre}}\big\}.$$

For simplicity of notation we assume that $q = p$ and $\lambda_{i,I}^{(k)} = r\lambda_{i,E}^{(k)}$, where $0 \leqslant r \leqslant 1$ is the ratio between inhibitory and excitatory inputs.

Furthermore we suppose that p_c out of p synapses carry the true signal and the rest of the $p - p_c$ synapses are noise (or distorted) signals. Synapses which code true signals are correlated, but synapses which code noise are independent. For simplicity of notation we assume that the correlation coefficient between the ith excitatory (inhibitory) synapse and the jth excitatory (inhibitory) synapse is a constant c, where $i, j = 1, \ldots, p_c$. The correlation considered here reflects the correlation of activity of different synapses, as discussed and explored in [9, 40]. More specifically, synaptic inputs take the following form ($p = q$):

$$\begin{aligned} I_{\mathrm{syn}}^{(k)}(t) &= a\sum_{i=1}^{p} E_i^{(k)}(t) - b\sum_{j=1}^{p} I_j^{(k)}(t) \\ &= a\sum_{i=1}^{p_c} E_i^{(k)}(t) + a\sum_{i=p_c+1}^{p} E_i^{(k)}(t) - b\sum_{i=1}^{p_c} I_i^{(k)}(t) - b\sum_{i=p_c+1}^{p} I_i^{(k)}(t) \end{aligned}$$

where $E_i^{(k)}(t), i = 1, \ldots, p_c$, are correlated Poisson processes with an identical rate $\lambda^{(k)}$ (signal), $E_i^{(k)}(t), i = p_c + 1, \ldots, p$, are Poisson processes with a firing rates λ_i independently and identically distributed random variables from $[0, \lambda_{\max}]$ Hz (noise), $I_i^{(k)}(t), i = 1, \ldots, p$, have the same properties as $E_i^{(k)}(t)$, but with a firing rate of $r\lambda^{(k)}$ or $r\lambda_i$ for $r \in [0, 1]$ representing the ratio between inhibitory and excitatory inputs. It was pointed out in [30] that the ratio of inhibitory and excitatory synapses is around 15/85. Of course, in general, inhibitory inputs are larger than excitatory inputs. All conclusions below can be easily extended to the case of $r > 1$. On the other hand, for simplicity of notation, we have introduced a single parameter r to describe the relationship between inhibitory and excitatory inputs. From the proofs below, we can see that this assumption can be easily relaxed. Without loss of generality we simply assume that $\lambda^{(1)}, \lambda^{(2)} \in [0, \lambda_{\max}]$ Hz.

Hence the neuron model receives two set of inputs: one is

$$a\sum_{i=1}^{p_c} E_i^{(1)}(t) + a\sum_{i=p_c+1}^{p} E_i^{(1)}(t) - b\sum_{i=1}^{p_c} I_i^{(1)}(t) - b\sum_{i=p_c+1}^{p} I_i^{(1)}(t)$$

where the signal term

$$a\sum_{i=1}^{p_c} E_i^{(1)}(t) - b\sum_{i=1}^{p_c} I_i^{(1)}(t)$$

is masked by the noise term

$$a\sum_{i=p_c+1}^{p} E_i^{(1)}(t) - b\sum_{i=p_c+1}^{p} I_i^{(1)}(t)$$

and the other is

$$a\sum_{i=1}^{p_c} E_i^{(2)}(t) + a\sum_{i=p_c+1}^{p} E_i^{(2)}(t) - b\sum_{i=1}^{p_c} I_i^{(2)}(t) - b\sum_{i=p_c+1}^{p} I_i^{(2)}(t)$$

where the signal term

$$a\sum_{i=1}^{p_c} E_i^{(2)}(t) - b\sum_{i=1}^{p_c} I_i^{(2)}(t)$$

is masked by the noise term

$$a\sum_{i=p_c+1}^{p} E_i^{(2)}(t) - b\sum_{i=p_c+1}^{p} I_i^{(2)}(t).$$

In the following, we further use diffusion approximations to approximate synaptic inputs [35] and assume $a = b$:

$$\begin{aligned} i_{\mathrm{syn}}^{(k)}(t) &= ap_c\lambda^{(k)}t + a\sum_{i=p_c+1}^{p}\lambda_i t - bp_c r\lambda^{(k)}t - b\sum_{i=p_c+1}^{p} r\lambda_i t \\ &\quad + \sqrt{(a^2+b^2r)\lambda^{(k)}p_c(1+c(p_c-1)) + (a^2+b^2r)\sum_{i=p_c+1}^{p}\lambda_i}\cdot B_t \\ &= a(1-r)t\left[p_c\lambda^{(k)} + \sum_{i=p_c+1}^{p}\lambda_i\right] \\ &\quad + a\sqrt{(1+r)\left[\lambda^{(k)}p_c(1+c(p_c-1)) + \sum_{i=p_c+1}^{p}\lambda_i\right]}\cdot B_t \end{aligned} \tag{2}$$

where B_t is the standard Brownian motion.

Therefore the term

$$a(1-r)t\left[p_c\lambda^{(k)} + \sum_{i=p_c+1}^{p}\lambda_i\right] \qquad k = 1, 2 \tag{3}$$

in equation (2) is the mean input signal to the cell. Without loss of generality, we always assume that $\lambda^{(1)} < \lambda^{(2)}$. Denote $p_k^{(\mathrm{in})}(\lambda)$ as the distribution density of random variables (ignore the constants $a(1-r)t$ in equation (3)).

$$p_c\lambda^{(k)} + \sum_{i=p_c+1}^{p}\lambda_i. \tag{4}$$

In summary, we consider the case that a neuron receives p synaptic inputs, with p_c out of p carrying the signals and $p - p_c$ being noise (distorted signals). The setup here roughly corresponds to the experiments of Newsome and his colleagues. We will explore this aspect in further publications [12].

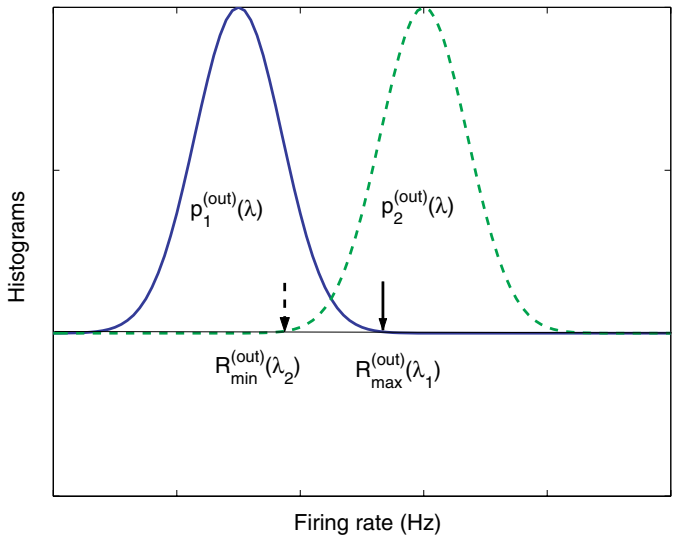

Figure 2. A schematic plot of two output histograms, $R_{\min}^{(\mathrm{out})}(\lambda_2)$ and $R_{\max}^{(\mathrm{out})}(\lambda^{(1)})$. As soon as $R_{\min}^{(\mathrm{out})}(\lambda_2) - R_{\max}^{(\mathrm{out})}(\lambda^{(1)}) > 0$, the two histograms are separable.

3. Discrimination capacity: the worst case

For a fixed $\lambda^{(1)} < \lambda^{(2)}$ we have two corresponding histograms $p_1^{(\mathrm{out})}(\lambda)$ and $p_2^{(\mathrm{out})}(\lambda)$ of output firing rates as shown in figure 2. Let

$$R_{\min}^{(\mathrm{out})}(\lambda^{(2)}) = \min\left\{\lambda : p_2^{(\mathrm{out})}(\lambda) > 0\right\}$$

and

$$R_{\max}^{(\mathrm{out})}(\lambda^{(1)}) = \max\left\{\lambda : p_1^{(\mathrm{out})}(\lambda) > 0\right\}$$

and denote

$$\alpha(\lambda^{(1)}, \lambda^{(2)}, c, r) = \left\{p_c : R_{\min}^{(\mathrm{out})}(\lambda^{(2)}) = R_{\max}^{(\mathrm{out})}(\lambda^{(1)})\right\}. \tag{5}$$

Hence for fixed $(\lambda^{(1)}, \lambda^{(2)}, c, r)$, $\alpha(\lambda^{(1)}, \lambda^{(2)}, c, r)$ gives us the critical value of p_c: when $p_c > \alpha(\lambda^{(1)}, \lambda^{(2)}, c, r)$ the input patterns are perfectly separable in the sense that the output firing rate histograms are not mixed; when $p_c < \alpha(\lambda^{(1)}, \lambda^{(2)}, c, r)$ the input patterns might not be separable. For fixed $\lambda^{(1)}, \lambda^{(2)}, c, r)$, α is termed the (*worst*) *discrimination capacity* of the neuron.

For input signals let us introduce more notation. Define

$$R_{\min}^{(\mathrm{in})}(\lambda^{(2)}) = \min\left\{\lambda : p_2^{(\mathrm{in})}(\lambda) > 0\right\}$$

and

$$R_{\max}^{(\mathrm{in})}(\lambda^{(1)}) = \max\left\{\lambda : p_1^{(\mathrm{in})}(\lambda) > 0\right\}.$$

Therefore as soon as $R_{\min}^{(\mathrm{in})}(\lambda^{(2)}) > R_{\max}^{(\mathrm{in})}(\lambda^{(1)})$ the two masked inputs are perfectly separable. Otherwise the two masked inputs are mixed. Hence the relationship between $R_{\min}^{(\mathrm{in})}(\lambda^{(2)}) - R_{\max}^{(\mathrm{in})}(\lambda^{(1)})$ and $R_{\min}^{(\mathrm{out})}(\lambda^{(2)}) - R_{\max}^{(\mathrm{out})}(\lambda^{(1)})$ characterizes the input–output relationship of the signals.

3.1. Behaviour of $\alpha(\lambda^{(1)}, \lambda^{(2)}, c, r)$

First of all, we note that the output firing rate is given by [35]

$$\langle T^{(k)} \rangle = \frac{2}{L} \int_{A(V_{\text{rest}}, \sum_{j=p_c+1}^{p} \lambda_j)}^{A(V_{\text{thre}}, \sum_{j=p_c+1}^{p} \lambda_j)} g(x)\, \mathrm{d}x \tag{6}$$

where

$$A(x, y) = \frac{xL - a[p_c\lambda^{(k)} + y](1-r)}{a\sqrt{[\lambda^{(k)} p_c(1 + c(p_c - 1)) + y](1+r)}}$$

and

$$g(x) = \left[\exp(x^2) \int_{-\infty}^{x} \exp(-u^2)\, \mathrm{d}u \right].$$

Let us define

$$\tilde{T}^{(k)}(x) = \frac{2}{L} \int_{A(V_{\text{rest}}, x)}^{A(V_{\text{thre}}, x)} g(u)\, \mathrm{d}u. \tag{7}$$

We know that the output firing rate is calculated via

$$1000/(\langle T^{(k)} \rangle + T_{\text{ref}})$$

where T_{ref} is the refractory period. It is obvious that $\tilde{T}(x)$ is a monotonic function of input $x \geqslant 0$, i.e. the output firing rate of a neuron is an increasing function of input. We conclude that $\alpha(\lambda^{(1)}, \lambda^{(2)}, c, r)$ is the solution of the following equation for p_c:

$$\begin{aligned} \int_0^{V_{\text{thre}}L} g\left(\frac{y - a[p_c\lambda^{(1)} + (p - p_c)\lambda_{\max}](1-r)}{a\sqrt{[\lambda^{(1)} p_c(1 + c(p_c - 1)) + (p - p_c)\lambda_{\max}](1+r)}} \right) \mathrm{d}y \\ = \frac{\sqrt{[\lambda^{(1)} p_c(1 + c(p_c - 1)) + (p - p_c)\lambda_{\max}]}}{\sqrt{[\lambda^{(2)} p_c(1 + c(p_c - 1))]}} \\ \times \int_0^{V_{\text{thre}}L} g\left(\frac{y - a(p_c\lambda^{(2)})(1-r)}{a\sqrt{[\lambda^{(2)} p_c(1 + c(p_c - 1))](1+r)}} \right) \mathrm{d}y. \end{aligned} \tag{8}$$

The critical value $\alpha(\lambda^{(1)}, \lambda^{(2)}, c, r)$ can be found analytically in the two most interesting cases: $c = 0$ and $r = 1$. Define

$$0 \leqslant \Lambda = \frac{\lambda^{(2)} - \lambda^{(1)}}{\lambda_{\max}} \leqslant 1.$$

We then have the following conclusions:

Theorem 1. *We assume* $\Lambda > 0, 0 < r < 1$,

- *When* $c > 0$ *we have*

$$\alpha(\lambda^{(1)}, \lambda^{(2)}, c, 1) < \alpha(\lambda^{(1)}, \lambda^{(2)}, 0, r) \tag{9}$$

and furthermore

$$\alpha(\lambda^{(1)}, \lambda^{(2)}, c, 1) = \frac{\sqrt{[\Lambda(1-c) + 1]^2 + 4pc\Lambda} - (1-c)\Lambda - 1}{2c\Lambda}. \tag{10}$$

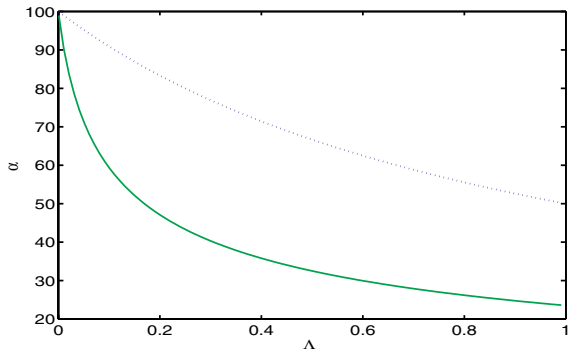

Figure 3. α versus Λ for $c = 0, r = 0$ (dotted line, independent of r according to theorem 1) and $c = 0.1, r = 1$ (solid line).

- *When* $c = 0$ *we have*

$$\alpha(\lambda^{(1)}, \lambda^{(2)}, 0, r) = \frac{p}{1 + \Lambda} \tag{11}$$

  independent of r.
- *When* $c < 0$ *we have*

$$\alpha(\lambda^{(1)}, \lambda^{(2)}, c, 1) > \alpha(\lambda^{(1)}, \lambda^{(2)}, 0, r). \tag{12}$$

The proof of theorem 1 is quite tricky and we postpone it to the appendix. In fact, from all our numerical results (see figure 4, bottom panel), we have the following stronger conclusions than theorem 1 (equations (9) and (12)).

- When $c > 0$ we have

$$\alpha(\lambda^{(1)}, \lambda^{(2)}, c, r_2) < \alpha(\lambda^{(1)}, \lambda^{(2)}, c, r_1) \tag{13}$$

  where $1 \geqslant r_2 > r_1 > 0$.
- When $c < 0$ we have

$$\alpha(\lambda^{(1)}, \lambda^{(2)}, c, r_2) > \alpha(\lambda^{(1)}, \lambda^{(2)}, c, r_1) \tag{14}$$

  where $1 \geqslant r_2 > r_1 > 0$.

However, we are not able to prove theoretically the stronger conclusions (equations (13) and (14)).

It is interesting to note that equations (11) and (10) are independent of a, V_{thre} and L, three essential parameters in the integrate-and-fire model. In other words, the results of equations (11) and (10) of the integrate-and-fire model are *universal*. In figure 3 we plot α versus Λ for $c = 0$ and $c = 0.1$ according to equations (11) and (10). For a given Λ and $c = 0.1$, the solid line in figure 3 gives us the smallest number of coherently synaptic inputs for an integrate-and-fire model to discriminate between input signals if we assume that $r \in [0, 1]$. Hence the solid line in figure 3 is the smallest discrimination capacity of an integrate-and-fire model with $c = 0.1$. It is worth pointing out that the lowest limit of α is about $\alpha = 23$. Finally we want to emphasize that our results are independent of input distributions. No matter what the input distribution is, as soon as p_c is greater than 40, the input signal can be perfectly separated from an observation of efferent spike trains provided that $\Lambda = 0.5$. The

improvement of discrimination capacity from $r = 0$ to $r = 1$ is remarkable, almost halving in most cases.

A universal result as in equations (10) and (11) above is illuminating since it is independent of model parameters and then widely applicable. However, the downside of such a result is that neurons modify their connections to improve their performance. Therefore we would argue that learning plays no role in improving its discrimination capacity, or discrimination tasks are not a primary computational task for a neuronal system. However, we want to point out that equation (10) is obtained for $r = 1$, the case with exactly balanced inhibitory and excitatory inputs. In a biologically realistic situation, neuron systems might operate in a region with $r < 1$. In the circumstances, α could depend on various model parameters and so learning might be important to improve the integrate-and-fire model discrimination capacity. Certainly to find a learning rule to improve neuronal discrimination capacity would be an interesting topic.

3.2. Input–output relationship

We first want to assess whether $R_{\min}^{(\mathrm{out})}(\lambda^{(2)}) - R_{\max}^{(\mathrm{out})}(\lambda^{(1)}) > 0$ even when $R_{\min}^{(\mathrm{in})}(\lambda^{(2)}) - R_{\max}^{(\mathrm{in})}(\lambda^{(1)}) < 0$, i.e. the input signal is mixed, but the output signal is separated. In figure 4 we plot $R_{\min}^{(\mathrm{out})}(\lambda^{(2)}) - R_{\max}^{(\mathrm{out})}(\lambda^{(1)})$ versus $R_{\min}^{(\mathrm{in})}(\lambda^{(2)}) - R_{\max}^{(\mathrm{in})}(\lambda^{(1)})$. It is easily seen that, after neuronal transformation, mixed signals are better separated when $c > 0$. For example, when $c = 0.1, r = 1$ and $R_{\min}^{(\mathrm{in})}(\lambda^{(2)}) - R_{\max}^{(\mathrm{in})}(\lambda^{(1)}) = -5000$ Hz (mixed), but $R_{\min}^{(\mathrm{out})}(\lambda^{(2)}) - R_{\max}^{(\mathrm{out})}(\lambda^{(1)}) > 0$ (separated). The conclusion is not true for $c = 0$, but the separation is not worse after neuronal transformation. In figure 4, it is clearly seen that when $r < 1$ and $c \neq 0$, the discrimination capacity depends on model parameters.

We can prove the following conclusions:

Theorem 2. *For the integrate-and-fire model*

- *if* $c > 0$ *we have*

  $R_{\min}^{(\mathrm{out})}(\lambda^{(2)}) - R_{\max}^{(\mathrm{out})}(\lambda^{(1)}) > 0 \qquad$ *when* $\quad R_{\min}^{(\mathrm{in})}(\lambda^{(2)}) - R_{\max}^{(\mathrm{in})}(\lambda^{(1)}) = 0$

- *if* $c = 0$ *we have*

  $R_{\min}^{(\mathrm{out})}(\lambda^{(2)}) - R_{\max}^{(\mathrm{out})}(\lambda^{(1)}) = 0 \qquad$ *when* $\quad R_{\min}^{(\mathrm{in})}(\lambda^{(2)}) - R_{\max}^{(\mathrm{in})}(\lambda^{(1)}) = 0$

- *if* $c < 0$ *we have*

  $R_{\min}^{(\mathrm{out})}(\lambda^{(2)}) - R_{\max}^{(\mathrm{out})}(\lambda^{(1)}) < 0 \qquad$ *when* $\quad R_{\min}^{(\mathrm{in})}(\lambda^{(2)}) - R_{\max}^{(\mathrm{in})}(\lambda^{(1)}) = 0.$

The conclusions above completely answer the question raised in the introduction. When $c > 0$, the output histograms become more separated than input histograms; when $c < 0$, the output histograms are more mixed than input histograms. $c = 0$ is the critical case.

4. Discrimination capacity: the distribution dependent case

Consider the random variable $\left(\sum_{i=p_c+1}^{p} \lambda_i\right)$ in equation (4) and let us denote $\left(\sum_{i=p_c+1}^{p} \lambda_i\right)_j$ as its jth sampling. We see that after m times of sampling, the smallest input signal would be

$$p_c\lambda^{(k)} + \left(\sum_{i=p_c+1}^{p} \lambda_i\right)_{(m)} \tag{15}$$

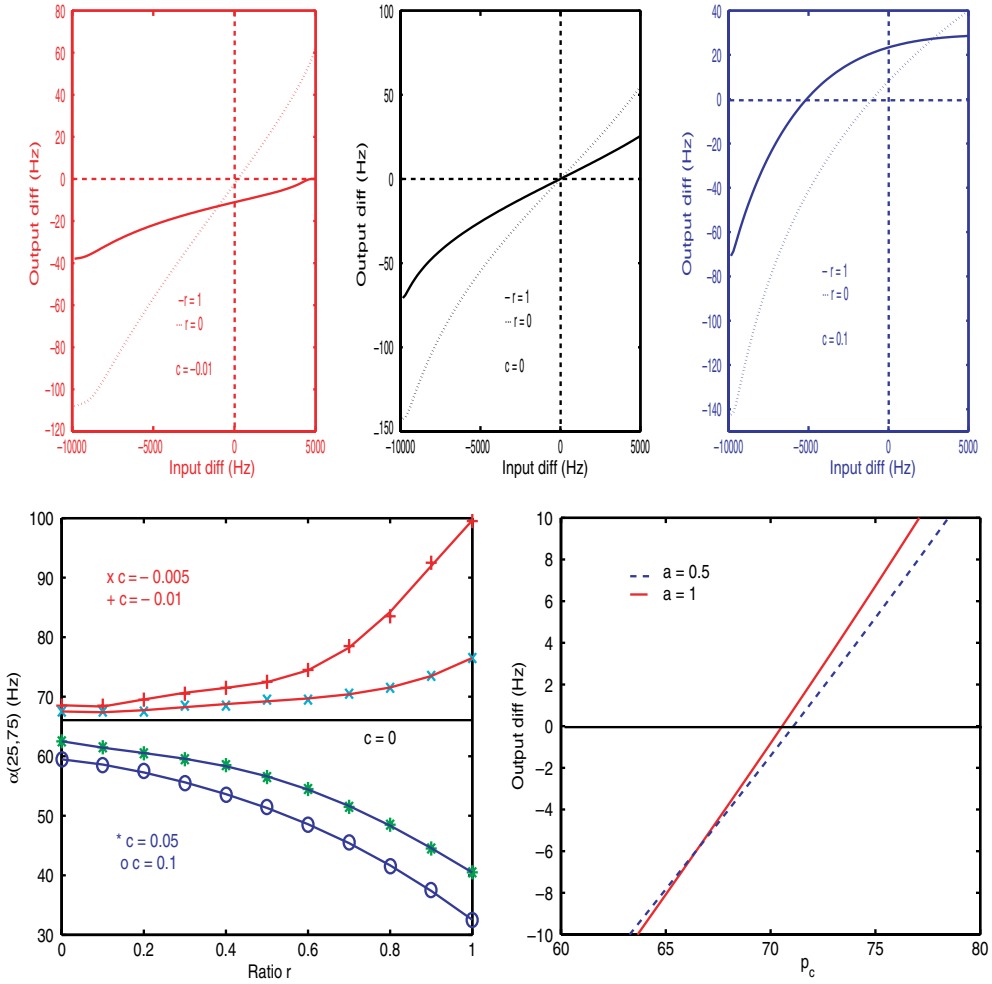

Figure 4. Upper panel, input difference $R_{\min}^{(\mathrm{in})}(\lambda^{(2)}) - R_{\max}^{(\mathrm{in})}(\lambda^{(1)})$ and output difference $R_{\min}^{(\mathrm{out})}(\lambda^{(2)}) - R_{\max}^{(\mathrm{out})}(\lambda^{(1)})$ for $c < 0$ (left), $c = 0$ (middle) and $c > 0$ (right). Output firing rates are equal to $1000/(\langle T^{(k)}\rangle + T_{\mathrm{ref}})$ with $T_{\mathrm{ref}} = 5$ ms. Bottom panel (left), numerical values are obtained by directly solving equation (8). Bottom panel (right), the dependence of the discrimination capacity on a with $r = 0.4$, $c = -0.01$.

and the largest would be

$$p_c\lambda^{(k)} + \left(\sum_{i=p_c+1}^{p} \lambda_i\right)^{(m)} \tag{16}$$

where $\left(\sum_{i=p_c+1}^{p} \lambda_i\right)^{(m)}$ and $\left(\sum_{i=p_c+1}^{p} \lambda_i\right)_{(m)}$ are the largest and smallest extreme values of the random variable $\left(\sum_{i=p_c+1}^{p} \lambda_i\right)$. Note that in section 3, we consider the worst cases and use 0 as the smallest input signal and $(p - p_c)\lambda_{\max}$ as the largest input signal.

We can carry out a rigorous analysis on the behaviour of the extreme values of the random variable $\left(\sum_{i=p_c+1}^{p} \lambda_i\right)$. However, the conclusion obtained will then depend on the actual distribution of λ_i. To avoid this, we then assume that $p \gg p_c, \lambda_i, i = p_c + 1, \ldots, p$, is an

identically and independently distributed random sequence (only for technical convenience) and we have

$$\left(\sum_{i=p_c+1}^{p}\lambda_i-(p-p_c)\langle\lambda_p\rangle\right)\Big/(\sqrt{p-p_c}\sigma(\lambda_p))\sim N(0,1)$$

where $\sigma(\lambda_p)=\sqrt{\langle\lambda_p^2\rangle-\langle\lambda_p\rangle^2}$.

We need the following lemma [21]:

Lemma 1. *For ξ_n being an identically and independently distributed normal sequence of random variables,*

$$P(a_m((\xi)^{(m)}-b_m)\leqslant x)\to\exp(-\exp(-x)) \tag{17}$$

where

$$\begin{cases}a_m=(2\log m)^{1/2}\\ b_m=(2\log m)^{1/2}-\frac{1}{2}(2\log m)^{-1/2}(\log\log m+\log(4\pi)).\end{cases} \tag{18}$$

Basically lemma 1 tells us that approximately $(\xi)_{(m)}$ diverges to positive (negative) infinity at a speed of b_m $(-b_m)$. We thus conclude that

$$\left(\sum_{i=p_c+1}^{p}\lambda_i\right)^{(m)}\sim\min\{[(p-p_c)\langle\lambda_p\rangle+\sqrt{p-p_c}\sigma(\lambda_p)(b_m)],(p-p_c)\lambda_{\max}\} \tag{19}$$

and

$$\left(\sum_{i=p_c+1}^{p}\lambda_i\right)_{(m)}\sim\max\{[(p-p_c)\langle\lambda_p\rangle-\sqrt{p-p_c}\sigma(\lambda_p)(b_m)],0\}. \tag{20}$$

We see that when $m\to\infty$, $\left(\sum_{i=p_c+1}^{p}\lambda_i\right)^{(m)}\to(p-p_c)\lambda_{\max}$ and $\left(\sum_{i=p_c+1}^{p}\lambda_i\right)_{(m)}\to 0$, which is the worst case we considered in the previous section.

For fixed $\lambda^{(1)}<\lambda^{(2)}$ and m, as before, we have two corresponding empirical histograms $p_1^{(\mathrm{out})}(\lambda,m)$ and $p_2^{(\mathrm{out})}(\lambda,m)$ of output firing rates. Let

$$R_{\min}^{(\mathrm{out})}(\lambda^{(2)},m)=\min\left\{\lambda,\,p_2^{(\mathrm{out})}(\lambda,m)>0\right\}$$

and

$$R_{\max}^{(\mathrm{out})}(\lambda^{(1)},m)=\max\left\{\lambda,\,p_1^{(\mathrm{out})}(\lambda,m)>0\right\}$$

and denote

$$\beta(\lambda^{(1)},\lambda^{(2)},c,r,m)=\left\{p_c:R_{\min}^{(\mathrm{out})}(\lambda^{(2)},m)=R_{\max}^{(\mathrm{out})}(\lambda^{(1)},m)\right\}. \tag{21}$$

Hence for fixed $(\lambda^{(1)},\lambda^{(2)},c,r,m)$, $\beta(\lambda^{(1)},\lambda^{(2)},c,r,m)$ gives us the critical value of p_c and we call it the discrimination capacity of the neuron (under m samplings).

4.1. Behaviour of $\beta(\lambda^{(1)},\lambda^{(2)},c,r,m)$

As in the previous section, we conclude that $\beta(\lambda^{(1)},\lambda^{(2)},c,r,m)$ is the solution of the following equation (p_c):

$$\int_0^{V_{\rm thre}L} g\left(\frac{y-a\left[p_c\lambda^{(1)}+\left(\sum_{i=p_c+1}^{p}\lambda_i\right)^{(m)}\right](1-r)}{a\sqrt{\left[\lambda^{(1)}p_c(1+c(p_c-1))+\left(\sum_{i=p_c+1}^{p}\lambda_i\right)^{(m)}\right](1+r)}}\right)\mathrm{d}y$$
$$=\frac{\sqrt{\left[\lambda^{(1)}p_c(1+c(p_c-1))+\left(\sum_{i=p_c+1}^{p}\lambda_i\right)^{(m)}\right]}}{\sqrt{\left[\lambda^{(2)}p_c(1+c(p_c-1))+\left(\sum_{i=p_c+1}^{p}\lambda_i\right)_{(m)}\right]}}$$
$$\times\int_0^{V_{\rm thre}L} g\left(\frac{y-a\left[p_c\lambda^{(2)}+\left(\sum_{i=p_c+1}^{p}\lambda_i\right)_{(m)}\right](1-r)}{a\sqrt{\left[\lambda^{(2)}p_c(1+c(p_c-1))+\left(\sum_{i=p_c+1}^{p}\lambda_i\right)_{(m)}\right](1+r)}}\right)\mathrm{d}y. \quad (22)$$

The critical value $\beta(\lambda^{(1)},\lambda^{(2)},c,r,m)$ can be analytically found in the two most interesting cases: $c=0$ and $r=1$. Define

$$0\leqslant\Theta=\frac{\lambda^{(2)}-\lambda^{(1)}}{\sigma(\lambda_p)}.$$

This corresponds to the parameter Λ defined in the previous section.

Theorem 3. *For* $\Theta>0$

- *when* $c>0$ *we have*
$$\beta(\lambda^{(1)},\lambda^{(2)},c,1,m)<\beta(\lambda^{(1)},\lambda^{(2)},0,r,m) \quad (23)$$
and furthermore $\beta=\beta(\lambda^{(1)},\lambda^{(2)},c,1,m)$ *is the solution of the equation*
$$\Theta\beta(1+c(\beta-1))=2\sqrt{p-\beta}b_m \quad (24)$$
provided that the approximations (19) and (20) are used.
- *When* $c=0$ *we have*
$$\beta(\lambda^{(1)},\lambda^{(2)},0,r,m)=\frac{2b_m\left[\sqrt{b_m^2+p\Theta^2}-b_m\right]}{\Theta^2} \quad (25)$$
independent of r, provided that the approximations (19) and (20) are used.
- *When* $c<0$ *we have*
$$\beta(\lambda^{(1)},\lambda^{(2)},c,1,m)>\beta(\lambda^{(1)},\lambda^{(2)},0,r,m). \quad (26)$$

Again from numerical simulations (see figures 6 and 8) we conclude the following.

- When $c>0$ we have
$$\beta(\lambda^{(1)},\lambda^{(2)},c,r_2,m)<\beta(\lambda^{(1)},\lambda^{(2)},c,r_1,m) \quad (27)$$
where $1\geqslant r_2>r_1>0$.
- When $c<0$ we have
$$\beta(\lambda^{(1)},\lambda^{(2)},c,r_2,m)>\beta(\lambda^{(1)},\lambda^{(2)},c,r_1,m) \quad (28)$$
where $1\geqslant r_2>r_1>0$.

Again it is interesting to note that equations (25) and (24) are independent of a, $V_{\rm thre}$ and L, three essential parameters in the integrate-and-fire model. In other words, the results of equations (25) and (24) of the integrate-and-fire model are *universal*. In figure 5 we plot β versus Θ for $c=0$ and $c=0.1$ according to equations (25) and (24). For a given Θ and $c=0.1$, the solid line in figure 5 gives us the smallest number of coherently synaptic inputs for an integrate-and-fire model to discriminate between input signals for $r\in[0,1]$. Hence the solid line in figure 5 is the smallest discrimination capacity of an integrate-and-fire model with $c=0.1$ if we assume that $r\in[0,1]$. It is worth pointing out that the lowest limit of β is about $\beta=14$.

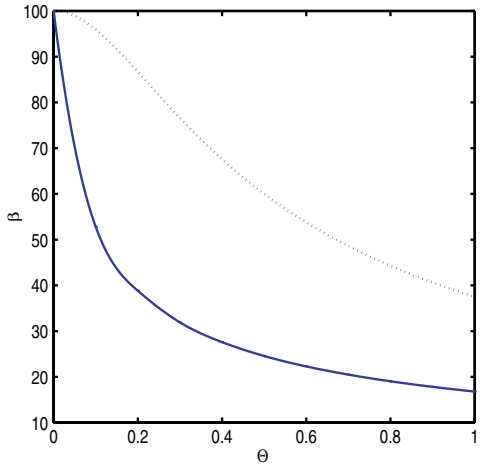

Figure 5. β versus Θ for $c = 0, r = 0$ (dotted line, independent of r according to theorem 3) and $c = 0.1, r = 1$ (solid line) with $m = 100$.

4.2. Input–output relationship

As before, we can assess the relationship between input and output histograms.

We can prove the following conclusions.

Theorem 4. *For the integrate-and-fire model,*

- *if* $c > 0$ *we have*

  $R^{(\mathrm{out})}_{\min}(\lambda^{(2)}, m) - R^{(\mathrm{out})}_{\max}(\lambda^{(1)}, m) > 0 \qquad$ *when* $\quad R^{(\mathrm{in})}_{\min}(\lambda^{(2)}, m) - R^{(\mathrm{in})}_{\max}(\lambda^{(1)}, m) = 0$

- *if* $c = 0$ *we have*

  $R^{(\mathrm{out})}_{\min}(\lambda^{(2)}, m) - R^{(\mathrm{out})}_{\max}(\lambda^{(1)}, m) = 0 \qquad$ *when* $\quad R^{(\mathrm{in})}_{\min}(\lambda^{(2)}, m) - R^{(\mathrm{in})}_{\max}(\lambda^{(1)}, m) = 0$

- *if* $c < 0$ *we have*

  $R^{(\mathrm{out})}_{\min}(\lambda^{(2)}, m) - R^{(\mathrm{out})}_{\max}(\lambda^{(1)}, m) < 0 \qquad$ *when* $\quad R^{(\mathrm{in})}_{\min}(\lambda^{(2)}, m) - R^{(\mathrm{in})}_{\max}(\lambda^{(1)}, m) = 0.$

5. Numerical results

Let us now consider the minimum total probability of misclassification (TPM) defined by

$$\mathrm{TPM} = \tfrac{1}{2}P(\text{misclassfied as } \lambda^{(2)} \,|\text{input is } \lambda^{(1)}) + \tfrac{1}{2}P(\text{misclassfied as } \lambda^{(1)} \,|\text{input is } \lambda^{(2)}).$$

For example, in figure 6, we see that TPM (in per cent) for the left upper panel is about 13.5% and for the right upper panel is 5.5%. Therefore adding inhibitory inputs to the neuron considerably improves its discrimination capability, reducing TPM from 13.5% to 5.5%.

The parameters used in simulating the IF model are $V_{\mathrm{thre}} = 20\,\mathrm{mV}$, $V_{\mathrm{rest}} = 0\,\mathrm{mV}$, $L = 1/20$, $a = b = 1\,\mathrm{mV}$, $p = 100$, $\lambda^{(1)} = 25$ Hz and $\lambda^{(2)} = 75$ Hz. A refractory period of 5 ms is added for all numerical results of efferent firing frequency. For each fixed set of parameters of the model, 100 spikes are generated to calculate each mean, standard deviation etc. The histograms are obtained using 100 firing rates, i.e. $m = 100$.

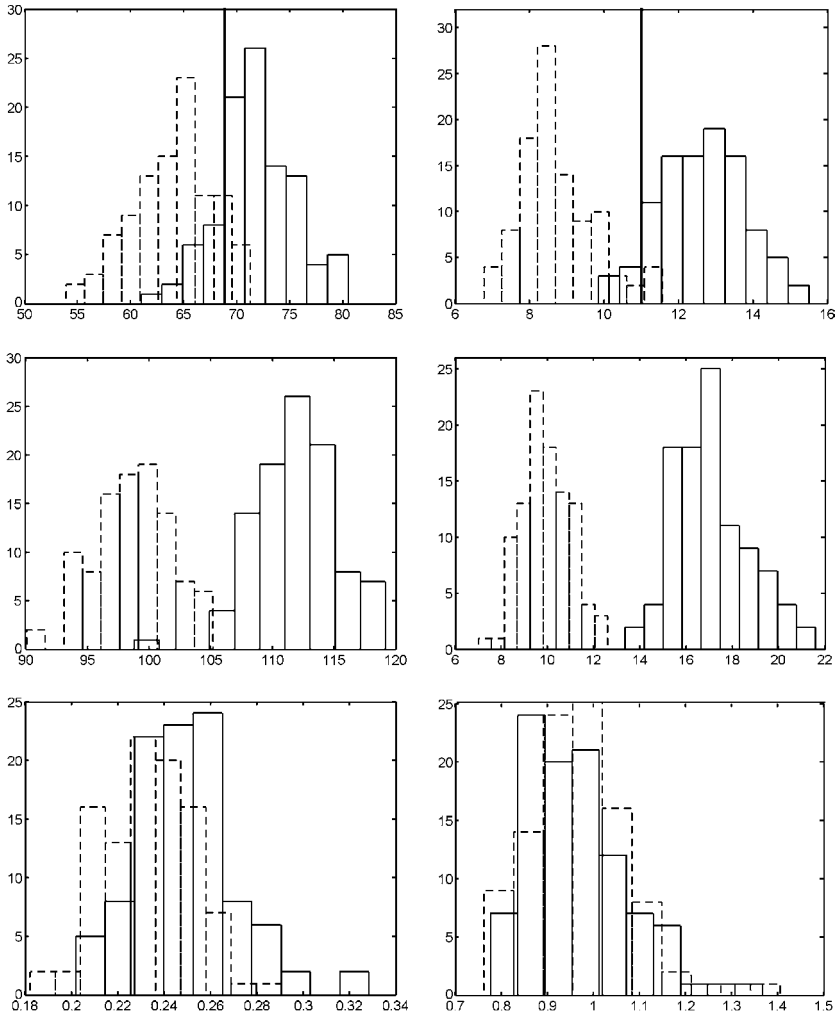

Figure 6. Upper and middle panels, histograms of firing rates (Hz) with $c = 0.1$ for the IF model. Left, exclusively excitatory inputs $r = 0$. Right, $r = 0.95$. Upper panels: $p_c = 15$. The minimum TPM is calculated according to the thick vertical lines (the optimal discrimination line). Middle panels: $p_c = 25$. Bottom panels: histograms of coefficient of variation (CV) for $p_c = 25$ and left with $r = 0$, right with $r = 0.95$, corresponding to the middle panels.

It is interesting to compare numerical results with theoretical results in the previous sections. From previous sections we have

$$\alpha(25, 75, 0.1, 1) = 32.5133$$

and

$$\beta(25, 75, 0.1, 1, 100) = 12.1251 \qquad \beta(0, 100, 0.1, 1, 100) = 7.8058.$$

From figure 8 (right) we conclude that the discrimination capacity would be between 15 and 20. The discrimination capacity from actual numerical simulations for $r = 1$ closes to $\beta(25, 75, 0.1, 1, 100)$.

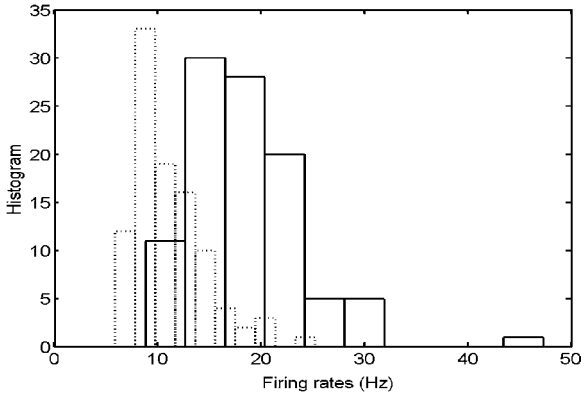

Figure 7. Histogram of firing rates (Hz) with $c = 0.1$ for the IF model, with identical parameters as in figure 6, bottom panel (right), but only 10 spikes are used for estimating mean firing rates.

Numerical simulations have been extensively carried out for the integrate-and-fire model and the IF–FHN model. All results are in agreement with our theoretical results in the previous sections and were reported in a meeting [10].

6. Discussion

We have considered the problem of discriminating between input signals in terms of an observation of efferent spike trains of a single integrate-and-fire neuron. We have demonstrated, both theoretically and numerically, that two key mechanisms to improve the discrimination capability of the model neuron are to increase inhibitory inputs and increase correlation between coherent inputs. Analytical results for two most interesting cases $c = 0$ and $r = 1$ are obtained and the results are independent of model parameters.

Our results offer answers to a few issues which were extensively discussed in the literature. We simply summarize two of them.

Increasing inhibitory inputs and increasing correlations between coherent inputs can enhance the discrimination capacity of a neuron. However, on the other hand we all know that increasing inhibitory inputs and correlations between inputs increases its output variability of efferent spike trains, which will simply broaden the efferent firing rate histograms and so reduce the discrimination capacity of a neuron. It seems our results in the current paper simply contradict this. Nevertheless, we must note that all theoretical results in sections 4 and 3 are obtained under the assumption that the efferent firing rates are exactly obtained. Results in section 5 clearly demonstrate that theoretical results in sections 4 and 3 are true even when the number of spikes used to obtain the firing rate histogram is small (100 spikes). In general our results reveal that a neuron system faces two opposite requirements: to obtain the mean firing rates as exactly as possible by reducing the variability of output spike trains (reducing inhibitory inputs and input correlations) and to increase the discrimination capacity by increasing inhibitory inputs and input correlations. To elucidate our points further, in figure 7, we plot the firing rate histograms, using the identical parameters as in figure 6 (middle panel, right), but with 10 spikes to estimate the mean, rather than 100 spikes. It is clearly shown that the firing rate histograms in figure 7 are less widely separated than those in figure 6, middle panel (right), and it is impossible to perfectly distinguish between two inputs. A neuronal

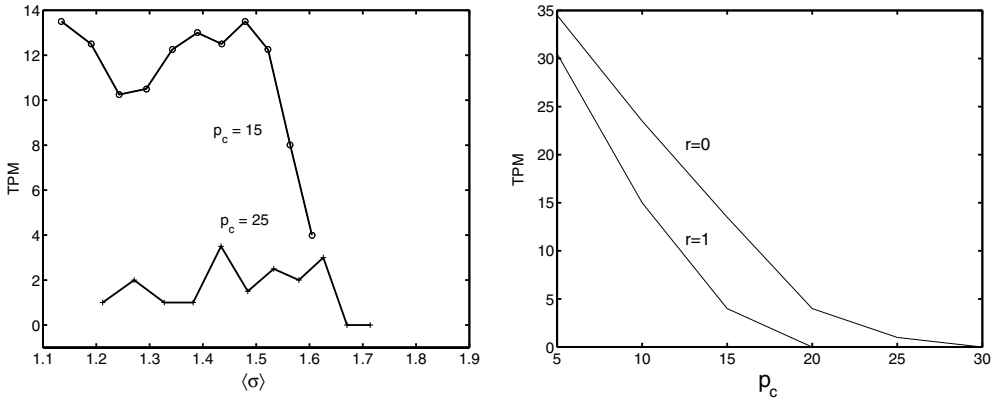

Figure 8. TPM% versus $\langle\sigma\rangle = \sqrt{a^2(1+r)\lambda^{(1)}p_c(1+c(p_c-1))+a^2(1+r)\sum_{i=p_c+1}^{p}\langle\lambda_i\rangle}$ with $\langle\lambda_i\rangle = 50$ Hz (left) and TPM versus p_c (right) for the IF model, $r \in [0, 1]$, $c = 0.1$, $\lambda^{(1)} = 25$ Hz. When $p_c = 15$ (left), it is clearly shown that TPM attains its optimal value at $r = 1$, i.e. the larger the noise, the better the discrimination (see the right-hand figure as well). All other parameters are the same as in section 5.

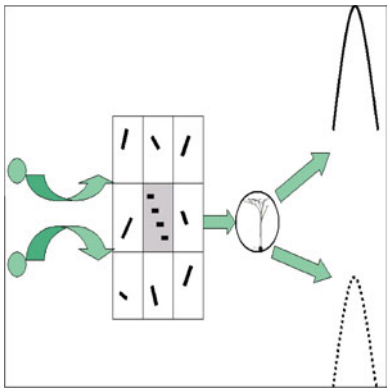

Figure 9. Correlations between coherent signals can be naturally introduced via neuronal pathways.

system must find a compromise way to resolve this issue. How to find an optimal trade-off between the two requirements is an interesting research topic.

Secondly, there are many publications arguing that there is an optimal value of noise at which a neuronal system can optimally extract information. Nevertheless, our results indicate that the optimal point is simply the one at which the neuron's output is most variable. We thus conclude that the larger the noise, the better for the neuron system (see the paragraph above and figure 8) to separate masked signals. This confirms the fact that noise is useful in a neural system, but not via the form of stochastic resonance.

The only assumption we introduced in the model is that coherent signals are more correlated than random signals. This seems a quite natural assumption given the structured cortical areas. Figure 9 illustrates the point. Coherent signals are transmitted by neurons grouping together (cortical columns) and neurons in the same column are bound to fire with a correlation. In contrast, noisy (distorted) signals are less correlated.

The integrate-and-fire model is the simplest model in theoretical neuroscience. One might easily argue that the model is too simple to be true for a realistic biological neuron.

Nevertheless, we have seen in the past few years that the integrate-and-fire model fits well with many experimental data (see, for example, [2, 14, 16]) and still serves as a canonical model of neurons. On the other hand, we have tested results in the current paper on other models as well [10]. It would be very interesting to investigate the impact of adaptation [7] and dynamical synapses [16] on discrimination tasks.

Currently we are also working on building up a system which mimics experiments carried out in [31, 23] etc with random dot stimuli and making judgments on dot moving directions [12].

Acknowledgments

We are grateful to the referee for his/her comments on the paper. JF was partially supported by grants from UK EPSRC (GR/R54569), (GR/S20574) and (GR/S30443), a grant of the Royal Society and an exchange grant between UK and China of the Royal Society.

Appendix

Proof of theorems

We only consider the case of $c > 0$. The case of $c < 0$ can be treated analogously

Lemma 2. *For fixed $y > 0$, $g(y/z)/z$ is a decreasing function of $z > 0$.*

Proof. Note that $g(x) > 0$,

$$\left(\frac{g(y/z)}{z}\right)' = \frac{-g'(y/z)y/z - g(y/z)}{z^2}$$

and the identity

$$g\prime(x) = 2xg(x) + 1$$

hence the conclusion follows.

We first prove theorem 2 for $c > 0$ and $r = 1$. Denote

$$\begin{aligned} A(p_c) &= \int_0^{V_{\text{thre}}L} g\left(\frac{y}{a\sqrt{[\lambda^{(1)}p_c(1+c(p_c-1))+(p-p_c)\lambda_{\max}]2}}\right)\mathrm{d}y \\ &= \frac{\sqrt{[\lambda^{(1)}p_c(1+c(p_c-1))+(p-p_c)\lambda_{\max}]}}{\sqrt{[\lambda^{(2)}p_c(1+c(p_c-1))]}} \\ &\quad\times \int_0^{V_{\text{thre}}L} g\left(\frac{y}{a\sqrt{[\lambda^{(2)}p_c(1+c(p_c-1))]2}}\right)\mathrm{d}y. \end{aligned} \tag{A1}$$

□

Lemma 3. *When $r > 0, c > 0$ we have*

$$R_{\min}^{(\text{out})}(\lambda^{(2)}) - R_{\max}^{(\text{out})}(\lambda^{(1)}) > 0 \qquad \textit{when} \quad R_{\min}^{(\text{in})}(\lambda^{(2)}) - R_{\max}^{(\text{in})}(\lambda^{(1)}) = 0.$$

Proof. We prove the conclusion for $r = 1$ first. Note that

$$R_{\min}^{(\text{in})}(\lambda^{(2)}) - R_{\max}^{(\text{in})}(\lambda^{(1)}) = 0$$

implies that

$$\lambda^{(2)} p_c = p_c \lambda^{(1)} + (p - p_c)\lambda_{\max}.$$

Hence

$$\lambda^{(2)} p_c + c\lambda^{(2)} p_c(p_c - 1) > p_c \lambda^{(1)} + (p - p_c)\lambda_{\max} + c\lambda^{(1)} p_c(p_c - 1).$$

For $y \geqslant 0$ according to lemma 2, we therefore have

$$\begin{aligned}
&\frac{1}{\sqrt{[\lambda^{(1)} p_c(1 + c(p_c - 1)) + (p - p_c)\lambda_{\max}]}} \\
&\qquad \times g\left(\frac{y}{a\sqrt{[\lambda^{(1)} p_c(1 + c(p_c - 1)) + (p - p_c)\lambda_{\max}]}}\right) \mathrm{d}y \\
&\qquad > \frac{1}{\sqrt{[\lambda^{(2)} p_c(1 + c(p_c - 1))]}}\, g\left(\frac{y}{a\sqrt{[\lambda^{(2)} p_c(1 + c(p_c - 1))]}}\right) \mathrm{d}y. \qquad \text{(A2)}
\end{aligned}$$

This fact, together with the fact that the function $A(p_c)$ is an increasing function of p_c, yields the conclusion that the intersection of $A(p_c)$ with $y = 0$ is on the left-hand side of $x = 0$ (see figure 4 upper panel, right) and so the conclusions of lemma 3 with $r = 1$ follow.

Now we turn our attention to the general case.

The key fact we employ in the proof is that the conclusions for the case of $r = 1$ are independent of the upper bound, i.e., $V_{\text{thre}}L$, of the integration. As in the case of $r = 1$

$$R^{(\text{in})}_{\min}(\lambda^{(2)}) - R^{(\text{in})}_{\max}(\lambda^{(1)}) = 0$$

implies that

$$\lambda^{(2)} p_c = p_c \lambda^{(1)} + (p - p_c)\lambda_{\max}.$$

Hence

$$\lambda^{(2)} p_c + c\lambda^{(2)} p_c(p_c - 1) > p_c \lambda^{(1)} + (p - p_c)\lambda_{\max} + c\lambda^{(1)} p_c(p_c - 1).$$

Therefore

$$\begin{aligned}
&\int_0^{V_{\text{thre}}L} g\left(\frac{y - a[p_c\lambda^{(1)} + (p - p_c)\lambda_{\max}](1 - r)}{a\sqrt{[\lambda^{(1)} p_c(1 + c(p_c - 1)) + (p - p_c)\lambda_{\max}](1 + r)}}\right) \mathrm{d}y \\
&\qquad - \frac{\sqrt{[\lambda^{(1)} p_c(1 + c(p_c - 1)) + (p - p_c)\lambda_{\max}]}}{\sqrt{[\lambda^{(2)} p_c(1 + c(p_c - 1))]}} \\
&\qquad \times \int_0^{V_{\text{thre}}L} g\left(\frac{y - a(p_c\lambda^{(2)})(1 - r)}{a\sqrt{[\lambda^{(2)} p_c(1 + c(p_c - 1))](1 + r)}}\right) \mathrm{d}y \\
&\quad = \int_{-a(p_c\lambda^{(2)})(1-r)}^{V_{\text{thre}}L - a(p_c\lambda^{(2)})(1-r)} g\left(\frac{y}{a\sqrt{[\lambda^{(1)} p_c(1 + c(p_c - 1)) + (p - p_c)\lambda_{\max}](1 + r)}}\right) \mathrm{d}y \\
&\qquad - \frac{\sqrt{[\lambda^{(1)} p_c(1 + c(p_c - 1)) + (p - p_c)\lambda_{\max}]}}{\sqrt{[\lambda^{(2)} p_c(1 + c(p_c - 1))]}} \\
&\qquad \times \int_{-a(p_c\lambda^{(2)})(1-r)}^{V_{\text{thre}}L - a(p_c\lambda^{(2)})(1-r)} g\left(\frac{y}{a\sqrt{[\lambda^{(2)} p_c(1 + c(p_c - 1))](1 + r)}}\right) \mathrm{d}y \\
&\quad = \left[\int_{-a(p_c\lambda^{(2)})(1-r)}^{\min\{V_{\text{thre}}L - a(p_c\lambda^{(2)})(1-r),\,0\}} + \int_0^{\max\{V_{\text{thre}}L - a(p_c\lambda^{(2)})(1-r),\,0\}}\right]
\end{aligned}$$

$$\times \left[g\left(\frac{y}{a\sqrt{[\lambda^{(1)} p_c(1+c(p_c-1))+(p-p_c)\lambda_{\max}](1+r)}} \right) \right.$$
$$- \frac{\sqrt{[\lambda^{(1)} p_c(1+c(p_c-1))+(p-p_c)\lambda_{\max}]}}{\sqrt{[\lambda^{(2)} p_c(1+c(p_c-1))]}}$$
$$\left. \times\, g\left(\frac{y}{a\sqrt{[\lambda^{(2)} p_c(1+c(p_c-1))](1+r)}} \right) \right] \mathrm{d}y. \tag{A3}$$

From the case of $r = 1$, we then assert that the term

$$\int_0^{\max\{V_{\text{thre}} L - a(p_c\lambda^{(2)})(1-r),0\}} [\cdot]\,\mathrm{d}y$$

is greater than zero. In the case of the term

$$\int_{-a(p_c\lambda^{(2)})(1-r)}^{\min\{V_{\text{thre}} L - a(p_c\lambda^{(2)})(1-r),0\}} [\cdot]\,\mathrm{d}y$$

we can change the variable from y to $-y$ and use the conclusions of $r = 1$ to show that it is also greater than zero. Furthermore, it is easily seen that

$$R_{\min}^{(\text{out})}(\lambda^{(2)}) - R_{\max}^{(\text{out})}(\lambda^{(1)}) < 0$$

when $p_c \to 0$.

Combining all conclusions above, we have proved theorem 2. □

Next we prove equations (11) and (10), i.e. theorem 1.

Lemma 4. *Equations (11) and (10) are the solution of*

$$p_c\lambda^{(1)} + (p - p_c)\lambda_{\max} = p_c\lambda^{(2)}$$

and

$$\lambda^{(1)} p_c(1 + c(p_c - 1)) + (p - p_c)\lambda_{\max} = \lambda^{(2)} p_c(1 + c(p_c - 1)).$$

Proof. In terms of lemma 2, the conclusions are obvious. □

Theorem 3 and theorem 4 can be proved similarly.

Finally we want to say a few words on the proof of the stronger version of the theorems. As above, we intend to assert that

$$R_{\min}^{(\text{out})}(\lambda^{(2)}) - R_{\max}^{(\text{out})}(\lambda^{(1)})$$

is an increasing function r when $\lambda^{(1)} p_c + (p - p_c)\lambda_{\max} > \lambda^{(2)} p_c$ (see figure 4, upper panel, right). Alternatively we can prove that $R_{\min}^{(\text{out})}(\lambda^{(2)}) - R_{\max}^{(\text{out})}(\lambda^{(1)}) = 0$ for $r = r_1$, but $R_{\min}^{(\text{out})}(\lambda^{(2)}) - R_{\max}^{(\text{out})}(\lambda^{(1)}) > 0$ for $r = r_2 > r_1$, as in lemma 3. However, when $r = r_1 > 0$, we do not have a clear-cut expression as in equation (11) and so we are not able to prove the stronger version.

References

[1] Abbott L F and Dayan P 1999 The effect of correlated variability on the accuracy of a population code *Neural Comput*. **11** 91–101

[2] Abbott L F, Varela J A, Sen K and Nelson S B 1997 Synaptic depression and cortical gain control *Science* **275** 220–3

[3] Barlow H 2001 Redundancy reduction revisited *Network* **12** 241–54

[4] Britten K H, Shadlen M N, Newsome W T, Celebrini S and Movshon J A 1992 The analysis of visual motion: a comparison of neuronal and psychophysical performance. *J. Neurosci*. **12** 4745–65

[5] Brown D, Feng J and Feerick S 1999 Variability of firing of Hodgkin–Huxley and FitzHugh–Nagumo neurons with stochastic synaptic input. *Phys. Rev. Lett*. **82** 4731–4

[6] Destexhe A, Rudolph M, Fellous J M and Sejnowski T J 2001 Fluctuating synaptic conductances recreate *in-vivo*-like activity in neocortical neurons *Neuroscience* **107** 13–24

[7] Fairhall AL *et al* 2002 Efficiency and ambiguity in an adaptive neural code *Nature* **412** 787–92

[8] Feng J 1997 Behaviours of spike output jitter in the integrate-and-fire model *Phys. Rev. Lett*. **79** 4505–8

[9] Feng J 2001 Is the integrate-and-fire model good enough?—a review *Neural Networks* **14** 955–75

[10] Feng J and Liu F 2002 A modelling study on discrimination tasks *Biosystems* **67** 67–73

[11] Feng J and Tirozzi B 2000 Stochastic resonance tuned by correlations in neuronal models. *Phys. Rev.* E **61** 4207–11

[12] Gaillared B 2002 Moving dots discrimination *Master Thesis* Sussex University

[13] Gerstner W and Kistler W 2002 *Spiking Neuron Models: Single Neurons, Populations, Plasticity* (Cambridge: Cambridge University Press)

[14] Leng G *et al* 2001 Responses of magnocellular neurons to osmotic stimulation involves co-activation of excitatory and inhibitory input: an experimental and theoretical analysis *J. Neurosci*. **21** 6967–77

[15] Gammaitoni L, Hänggi P, Jung P and Marchesoni F 1998 Stochastic resonance *Rev. Mod. Phys*. **70** 224–87

[16] Goldman M S, Maldonado P and Abbott L F 2002 Redundancy reduction and sustained firing with stochastic depressing synapses *J. Neurosci*. **22** 584–91

[17] Gray C M, Koenig P, Engel A K and Singer W 1989 Oscillatory responses in cat visual cortex exhibit inter-columnar synchronization which reflects global stimulus properties *Nature* **338** 334–7

[18] Kast B 2001 Decisions, decisions *Nature* **411** 126–8

[19] Kreiter A K and Singer W 1996 Stimulus-dependent synchronization of neuronal responses in the visual cortes of the awake macaque monkey *J. Neurosci*. **16** 2381–96

[20] Laughlin S B 1981 A simple coding procedure enhances a neuron's information capacity *Z. Naturforsch*. **36c** 910–2

[21] Leadbetter M R, Lindgren G and Rootzén H 1983 *Extremes and Related Properties of Random Sequences and Processes* (New York: Springer)

[22] Longtin A, Moss F and Bulsara A 1991 Time interval sequences in bistable systems and noise induced transmission of neural information *Phys. Rev. Lett*. **67** 656–9

[23] Parker A J and Newsome W T 1998 Sense and the single neuron: probing the physiology of perception *Ann. Rev. Neurosci*. **21** 227–77

[24] Petersen R S, Panzeri S and Diamond M E 2001 Population coding of stimulus location in rat somatosensory cortex *Neuron* **32** 503–14

[25] Petersen R S, Panzeri S and Diamond M E 2002a Population coding in somatosensory cortex *Curr Opin Neurobiol*. **12** 441–7

[26] Rieke F, Warland D, de Ruyter van Steveninck R and Bialek W 1997 *Spikes* (Cambridge, MA: MIT Press)

[27] Romo R and Salinas E 2001 Touch and go: decision mechanisms in somatosensation. *Ann. Rev. Neurosci*. **24** 107–37

[28] Rudolph M and Destexhe A 2001 Do neocortical pyramidal neurons display stochastic resonance? *J. Comput. Neurosci*. **11** 19–42

[29] Rudolph M and Destexhe A 2001 Correlation detection and resonance in neural systems with distributed noise sources, *Phys. Rev. Lett*. **86** 3662–5

[30] Shadlen M N and Newsome W T 1994 Noise, neural codes and cortical organization, *Curr. Opin. Neurobiol*. **4** 569–79

[31] Shadlen M N and Newsome W T 1996 Motion perception: seeing and deciding *P. Natl. Acad. Sci. USA* **93** 628–33

[32] Salinas E and Sejnowski TJ 2001 Correlated neuronal activity and the flow of neural information *Nat. Rev. Neurosci*. **2** 539–50

[33] Salinas E and Sejnowski T J 2000 Impact of correlated synaptic input on output firing rate and variability in simple neuronal models *J. Neurosci*. **20** 6193–209

[34] Sompolinsky H *et al* 2001 Population coding in neuronal systems with correlated noise *Phys. Rev.* E **64** 051904
[35] Tuckwell H C 1988 *Introduction to Theoretical Neurobiology* vol 2 (Cambridge: Cambridge University Press)
[36] Bezzif M, Diamond M E and Treves A 2002 Redundancy and synergy arising from pairwise correlations in neuronal ensembles *J. Comput. Neurosci.* **12** 165–74
[37] Usrey W M and Reid R C 1999 Synchronous activity in the visual system *Ann. Rev. Physiol.* **61** 435–56
[38] van Vereeswijk C, Abbott L F and Ermentrout G B 1994 When inhibition not excitation synchronizes neural firing *J. Comput. Neurosci.* **1** 313–21
[39] van Vreeswijk C and Sompolinsky H 1996 Chaos in neuronal networks with balanced excitatory and inhibitory activity *Science* **274** 1724–6
[40] Zohary E, Shadlen M N and Newsome W T 1994 Correlated neuronal discharge rate and its implications for psychophysical performance *Nature* **370** 140–3
[41] Stevens C F and Zador A M 1998 Input synchrony and the irregular firing of cortical neurons *Nat. Neurosci.* **1** 210–7